THE ARCHIVE OF MECHANICAL ENGINEERING

Vol. LII 2005 Number 3

Key words: *spruce wood, knots, biaxial testing, single-surface plasticity, finite element simulation*

*HERBERT W. MÜLLNER**), *MARTIN FLEISCHMANN**), *JOSEF EBERHARDSTEINER**)

ORTHOTROPIC SINGLE-SURFACE PLASTICITY MODEL FOR SPRUCE WOOD INCLUDING THE EFFECT OF KNOTS

Finite element simulations of structures and structural details require suitable material models. Today there is still a lack of such constitutive material models in timber engineering. Therefore, a perennial research project at the Institute for Mechanics of Materials and Structures at the Vienna University of Technology was performed. In this paper the testing equipment, the experiments, the developed material model and its implementation in finite element software will be explained. One focus of the mentioned project is the acquisition of the mechanical behaviour of biaxially, oblique to fibre direction loaded spruce wood. This enables a better simulation of multiaxial stress states in real timber structures. The applicability of the implemented constitutive model will be demonstrated by means of a nonlinear finite element analysis of a bone-shaped test specimen.

1. Introduction

For the development of a constitutive material model for spruce wood, different types of experiments are required. During the 1990's, a test series on clear spruce wood subjected to biaxial states of stress has been performed. These tests were designed for the investigation of stress states with their principal directions being oblique to the longitudinal and radial direction of wood. In 2003 and 2004, additional tests were performed filling up the lack of experimental information with respect to the tangential material direction and knots.

The knowledge of the mechanical behaviour of the principal material directions as well as of the influence of knots on the strength properties are necessary for realistic finite element ultimate load analyses of multiaxial

*) *Institute for Mechanics of Materials and Structures, Vienna University of Technology, Vienna, Austria; E-mail:* Herbert.Muellner@tuwien.ac.at; ej@imws.tuwien.ac.at

loaded structural details as well as of structures made of wood. Uniaxial experiments in different material directions with knots to determine the stiffening properties of wood were performed, too. Results of these tests and consideration of its results in an orthotropic material model will be presented and discussed in this contribution.

Figure 1 gives an overview of the necessary tasks for the desired material model. For the labelling of the principal material directions L, R and T see Fig. 3(a).

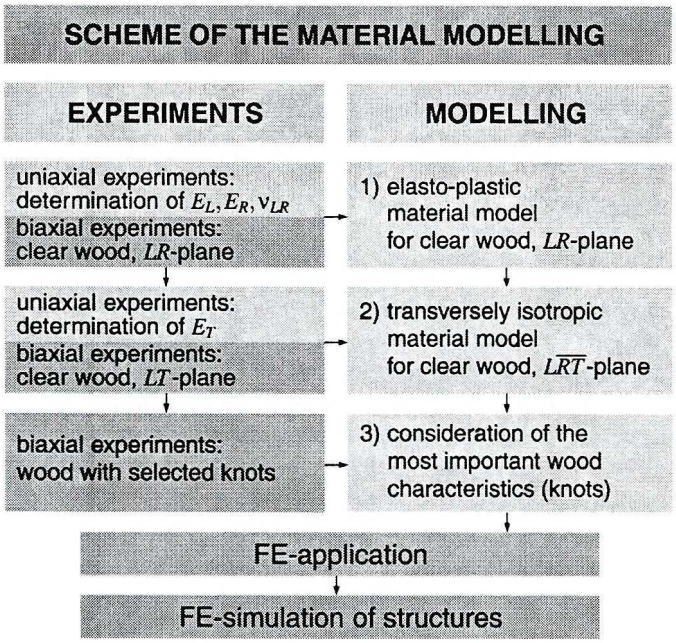

Fig. 1. Development of a plasticity model for wood

2. Experimental investigation of spruce wood under biaxial loading

Constitutive modelling of the biaxial mechanical behaviour of solid wood requires knowledge of both the stress-strain relations in the pre-failure domain, as well as the failure locations for arbitrary strain paths. Both requirements were satisfied in a comprehensive test series carried out by EBERHARDSTEINER [1].

2.1. Biaxial testing machine and the contactless deformation analysis system

The developed testing equipment, described in detail in [1], consists of a biaxial servo-hydraulic testing device for anisotropic materials and of a 3D

Electronic Speckle Pattern Interferometer (3D ESPI) for three-dimensional contactless full-field deformation analysis. The latter was used to measure the incremental in-plane deformations and its distribution in the central region of the specimen. Based on the obtained displacement field the state of strain and the strain history were determined by numerical differentiation.

The thickness t of the specimen's measuring area (140×140 mm) has been chosen to be 4.5 mm for states of biaxial tension and combined tensile and small compressive stresses. In order to prevent buckling of the specimen, biaxial compression tests were performed on specimens with $t = 7.5$ mm and 9.5 mm. The prescribed displacements were applied by means of 24 servo-hydraulic devices applied to the 12 loading points as shown in Figs. 2(a) and (b). This enables individual control of the in-plane position for each of the loading points with an accuracy of 2–3 μm.

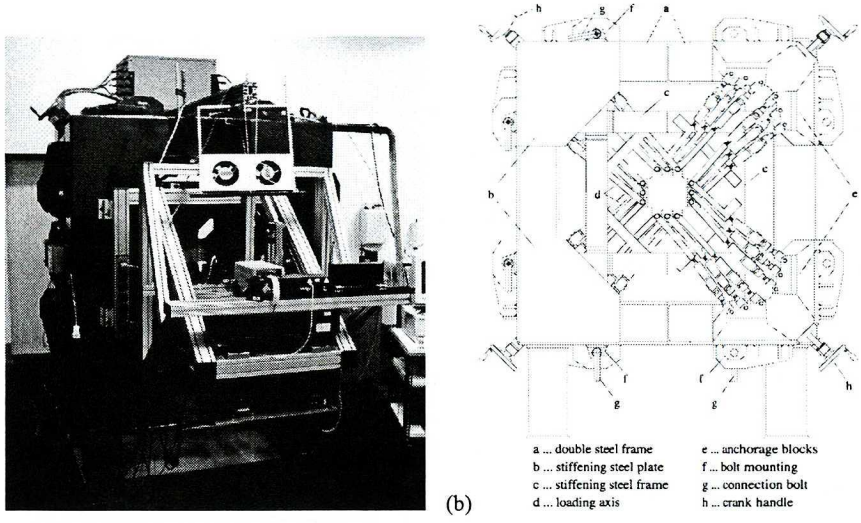

Fig. 2. Biaxial testing device

2.2. Test specimen

Filling the gap on biaxial strength tests in the *LR*-plane, as well as the measurement of the stress-strain behaviour under biaxial loading in the pre-failure domain, were the design goals for a novel experiment by EBERHARDSTEINER [1].

With a constant moisture content of $u = 12\%$ (standard climate: $T = +20°C$ and $RH = 65\%$), a series of approximately 500 displacement-driven biaxial strength tests were performed. These tests cover the whole set of distinguish-

able stress states for an orthotropic material under plane stress conditions in the *LR*-plane as well as in the *LT*-plane. *L* denotes the longitudinal or fibre direction, *R* is the radial direction, and *T* is the tangential direction within the stem of a tree (see Fig. 3(a)). The influence of knots on the strength properties was investigated by means of approximately 50 experiments done by FLEISCHMANN et al. [2]. In addition to the proportional biaxial strength tests, a small number of tests with loading-unloading-reloading cycles at different displacement levels was performed, too.

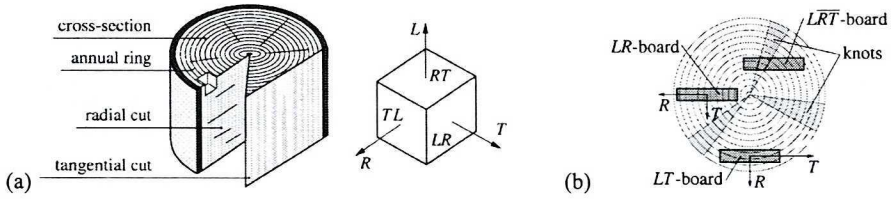

Fig. 3. Part of a stem of a tree (a) principal material directions, (b) location of test material

The individual tests are characterised by two mechanical parameters:

- *grain angle* φ – it is the angle between principal loading direction and fibre direction.
- *displacement ratio* κ – it is defined as $\kappa = \bar{u}:\bar{v}$, with $\bar{u}$ and $\bar{v}$ as the displacement vectors at the middle load application point of each border of the specimen, according to Fig. 4(a).

Most of the displacement-driven experiments were characterized by a proportional stepwise loading until fracture was reached. The displacement steps applied at each of the 12 discrete load application points of the specimen varied from 4 to 10 μm. To apply biaxial loading, a cruciform specimen is used (type "A", see Fig. 4(a)). In addition, a modified specimen for uniaxial experiments with wood characterised by selected knots is used (type "B", see Fig. 4(b)).

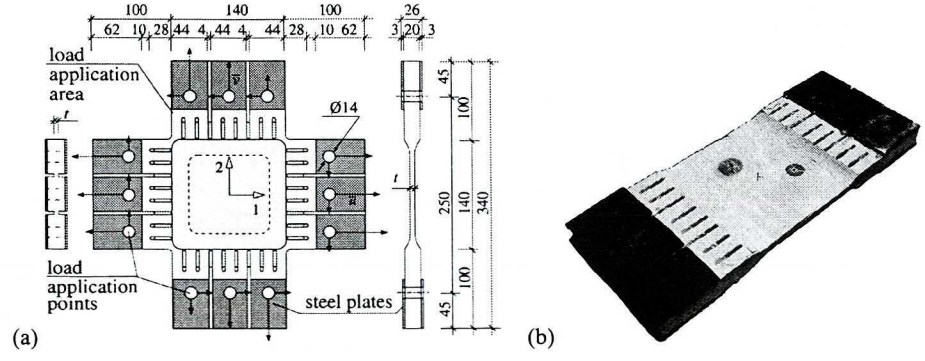

Fig. 4. Test specimen (a) cruciform version type "A", (b) modified version type "B"

Figure 5, e.g., refers to all experiments performed at a grain angle of $\varphi = 0°$ and 30°, respectively. The axis values are the principal stresses, σ_1 and σ_2, which are aligned with the horizontal and vertical axis of the test specimen. Each line represents the stress path obtained from a single test under proportionally increasing prescribed displacements. The symbol at the end of each line indicates the end of the elastic behaviour, which has been defined as the end of the linear part of the respective stress-strain relationship.

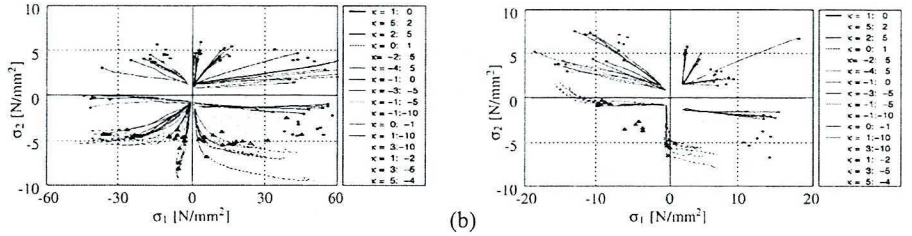

Fig. 5 Biaxial strength data and evolution of principal stress ratio σ_2/σ_1 (a) for grain direction $\varphi = 0°$ and various displacement ratios κ (b) for grain direction $\varphi = 30°$ and various displacement ratios κ

A verification of the suggested material model for plane stress states by means of back-calculations of the biaxial experiments by EBERHARDSTEINER [1] was done by MÜLLNER et al. [4]. The performed simulations of the mentioned experiments show a good agreement between the model and the test results for most modes of biaxial loading.

3. Analysis of experiments and development of a material model

Following Fig. 1, the development of a constitutive material model was done in three steps.

3.1. *LR*-plane of clear spruce wood

The properties and the concept of the used single-surface plasticity model are summarised in MÜLLNER et al. [4]. This material model can be used for the simulation of clear spruce wood under various biaxial in-plane stresses. The extension of the material model for consideration of transverse shear stresses is described in MÜLLNER et al. [5]. The formulation of a non-associated hardening and softening rule allows the consideration of several modes of failure identified from the results of the experimental investigation. The basis of the single-surface material description is the elliptic yield condition by TSAI & WU [6] as:

$$f(\boldsymbol{\sigma}, \mathbf{p}) = a_{LL}\sigma_L + a_{RR}\sigma_R + b_{LLLL}\sigma_L^2 + b_{RRRR}\sigma_R^2 + b_{LLRR}\sigma_L\sigma_R + 4b_{LRLR}\tau_{LR}^2 - 1 = 0, \tag{1}$$

which is shown in Fig. 6.

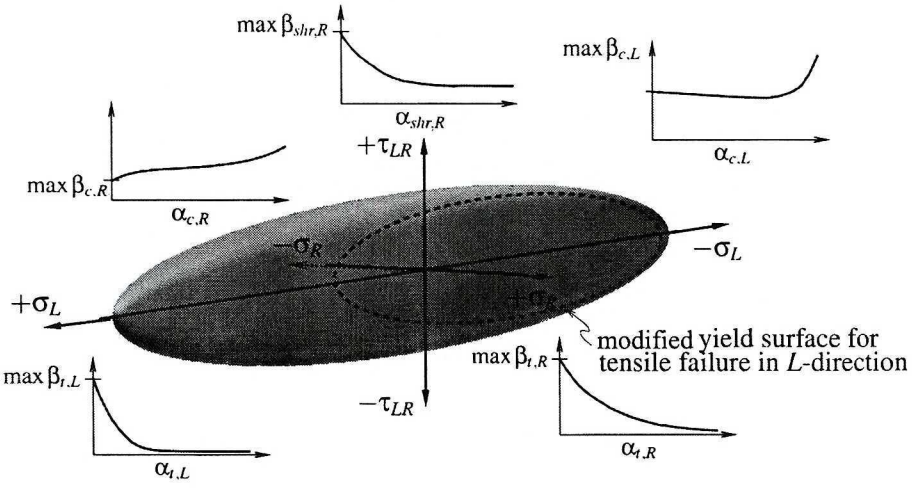

Fig. 6. Yield surface of single-surface material model in the orthotropic stress space and evolution laws for the strength values depending on the strain-like primary variables a_i

The formulation of five evolution laws, as shown in Fig. 6, requires five control variables. These so-called primary variables are collected in a vector $\boldsymbol{\alpha}$. The determination of a is subject to $\boldsymbol{\alpha}$ non-associated hardening and softening rule. This rule considers the different modes of failure which were identified as:

- brittle tensile failure in fibre direction,
- compressive failure with densification in fibre direction,
- brittle tensile failure perpendicular to grain, and
- ductile compressive behaviour with densification perpendicular to grain.

At large deformations, both compressive modes, show a phenomenon called *densification*, where the strength rises and the material becomes almost rigid [3]. This effect is also considered in the material model.

In order to obtain a uniquely invertable relation between the six parameters a_{ij} and b_{ijkl} $(i,j,k,l = \{L,R\})$ of (1) and the five strength values according to the five evolution laws, the latter have to be enriched by the constraint tan ϕ_0^*. For more details see MÜLLNER et al. [4].

3.2. *LT*-plane of clear spruce wood

According to the different experiments, an extension of the material model for the mechanical behaviour of spruce wood in the tangential

direction was done. The cross sections of boards and beams, which are widely used in timber engineering, are characterised by fibre orientations in R- as well as in T-direction. By contemplating a cross-section of a board both the R- and T-quotas are available (see Fig. 7(b)).

To determine these quotas a characteristic cross-section of a gluelam beam is used. The analysis will be carried out according to Figs. 7(a) and 7(b).

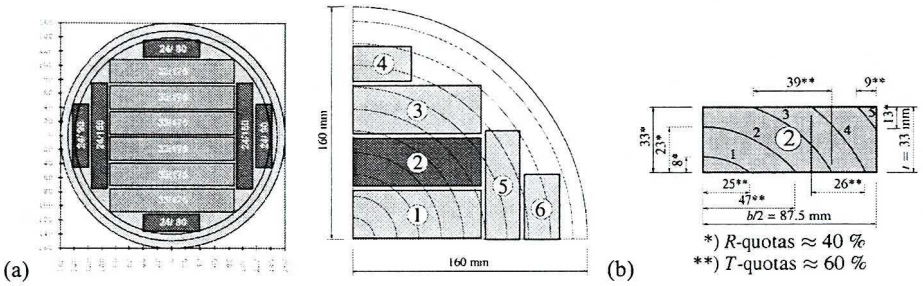

Fig. 7. Distribution of annular rings in a quarter of a stem for the production of gluelam beams (a) characteristic cross-section, (b) determination of the R- and T-quotas for board No. 2

Figures 8(a) and 8(b) show characteristic stress-strain curves which compare the mechanical behaviour for wood in R- and in T-direction. Compared to the L-direction, the material behaviour in R- and T-direction is rather similar.

Therefore, it is possible to reduce the mechanical behaviour in R- and T-direction to a $\overline{RT}$-equivalent. This fact leads to the use of the same transversely isotropic material model as for the LR-plane in the elastic region for spruce wood. In comparison to European design codes, two principal material directions (at a grain angle of 0° and 90°) are used, too.

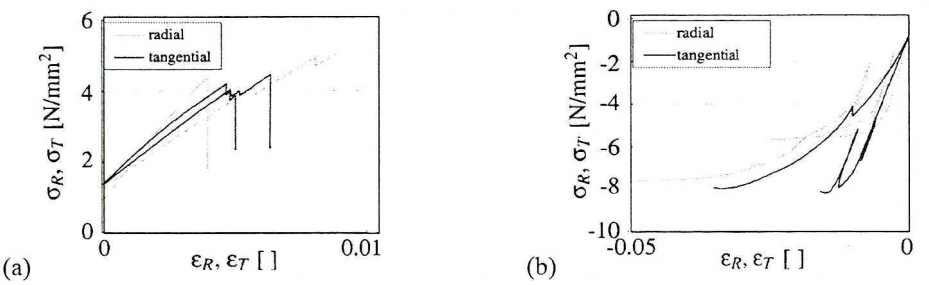

Fig. 8. Characteristic stress-strain curves for (a) tensile and (b) compressive loading in R- and T-direction

Using a non-linear regression analysis, the interpretation of all experiments according to Section 2.2 leads to the following material parameters

according for the criterion by TSAI & WU [6]. By changing the subscripts from R to $\overline{RT}$ the material parameters in (1) for the material directions L, R and T are obtained. They are collected in the vector

$$\mathbf{p} = \begin{Bmatrix} a_{LL} \\ a_{\overline{RT}\,\overline{RT}} \\ b_{LLLL} \\ b_{\overline{RT}\overline{RT}\overline{RT}\overline{RT}} \\ b_{LL\overline{RT}\overline{RT}} \\ b_{L\overline{RT}L\overline{RT}} \end{Bmatrix} = \begin{Bmatrix} -0.006394\,\text{mm}^2/\text{N} \\ +0.029990\,\text{mm}^2/\text{N} \\ +0.000333\,\text{mm}^4/\text{N} \\ +0.045750\,\text{mm}^4/\text{N} \\ +0.000051\,\text{mm}^4/\text{N} \\ +0.005009\,\text{mm}^4/\text{N} \end{Bmatrix}, \quad \mathbf{R}_y^0 = \begin{Bmatrix} \max \beta_{t,L}^0 \\ \max \beta_{c,L}^0 \\ \max \beta_{t,\overline{RT}}^0 \\ \max \beta_{c,\overline{RT}}^0 \\ \tan \phi_0^* \\ \max \beta_{shr,\overline{RT}}^0 \end{Bmatrix} = \begin{Bmatrix} 65.4\,\text{N/mm}^2 \\ 46.1\,\text{N/mm}^2 \\ 4.4\,\text{N/mm}^2 \\ 5.1\,\text{N/mm}^2 \\ -0.001126 \\ 7.2\,\text{N/mm}^2 \end{Bmatrix} \tag{3}$$

is a vector containing the five maxima of the initial (superscript "0") strength values, $\max \beta_{i,j}^0$ ($i = \{t,c\}$, $j = \{L, \overline{RT}\}$) and $\max \beta_{shr\overline{RT}}^0$, as well as the initial inclination $\tan \phi_0^*$ of the yield surface in the plane $\tau_{L\overline{RT}} = 0$. Further details can be found in MÜLLNER et al. [4]. Using the linear regression equations published in EBERHARDSTEINER [1], the average elastic material parameters for all accomplished experiments can be obtained as summarized in Table 1.

Table 1.

Elastic material parameter set for an average density of $\rho = 0.44$ g/cm³

$E_L = 13000$ N/mm²	$E_{\overline{RT}} = 560$ N/mm²
$\nu_{L\overline{RT}} = 0.50$	$G_{L\overline{RT}} = 520$ N/mm²

3.3. Consideration of significant wood properties

Because knots are a commanding criterion of wood, the material model was extended by the influence of knots on the strength values which are used in the material model. This fact is inseparably combined with the deviation of the fibre direction in the vicinity of knots. For this reason, a dimensionless knot factor *ksa* (knotsumarea ratio) has been defined. The knot factor can be included in the software of automatically working grading machines used in the timber industry. *ksa* is calculated as follows:

$$ksa = \frac{\sum_{i=1}^{m} k_i + s \cdot \sum_{j=1}^{n} ek_j}{2 \cdot b}, \tag{4}$$

where k_i is the width of a single knot, ek_j is the width of an edge knot, s is an experimental determined increasing factor for edge knots and b is the width of the considered board. Figures 9(a) and (b) gives an explanation of the mentioned values for a LT-board.

Fig. 9. Cross-section of a board (a) without edge knots, (b) with edge knots

Experiments by means of specimens shown in Fig. 4(b) were carried out in order to determine the influence of knots on the different uniaxial strength properties of wood. It will be considered by means of changing size of the elliptical yield surface. For instance, the tensile strength in longitudinal direction will be reduced by means of the following law:

$$\max \beta^0_{t,L}(ksa) = \max \beta^0_{t,L} \cdot e^{-2.82 \cdot ksa}. \tag{5}$$

Figure 10(a) shows the determination of the exponent in (5) by means of the mentioned experiments, and Fig. 10(b) shows the influence of a knot factor of 20% on the size of the initial yield surface.

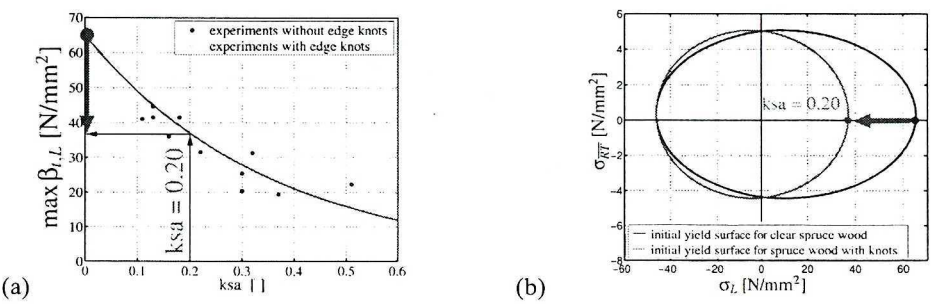

Fig. 10. Influence of knots and local fibre deviations (a) reduction of the tensile strength in longitudinal direction, (b) difference of the yield surface for wood with and without knots

Investigations for the other principal directions of wood have also been carried out. The influence of *ksa* on these strength values is implemented in a similar way as shown in this section. As against the strength properties, the

influence of knots and local fibre deviations around knots on the stiffness properties, i. e. elastic material parameters, will be neglected.

4. Comparison experiment – finite element simulation

In order to verify the performance of the developed material model, it is necessary to compare experimental and numerical results. As a first example a bone-shaped specimen is tested. The displacement driven compression experiment is performed inclined to the fibre direction. The reference configuration in the biaxial testing machine and the dimensions of the test specimen are shown in Fig. 11(a). The testing device has been compressed at a range of 2.5 mm.

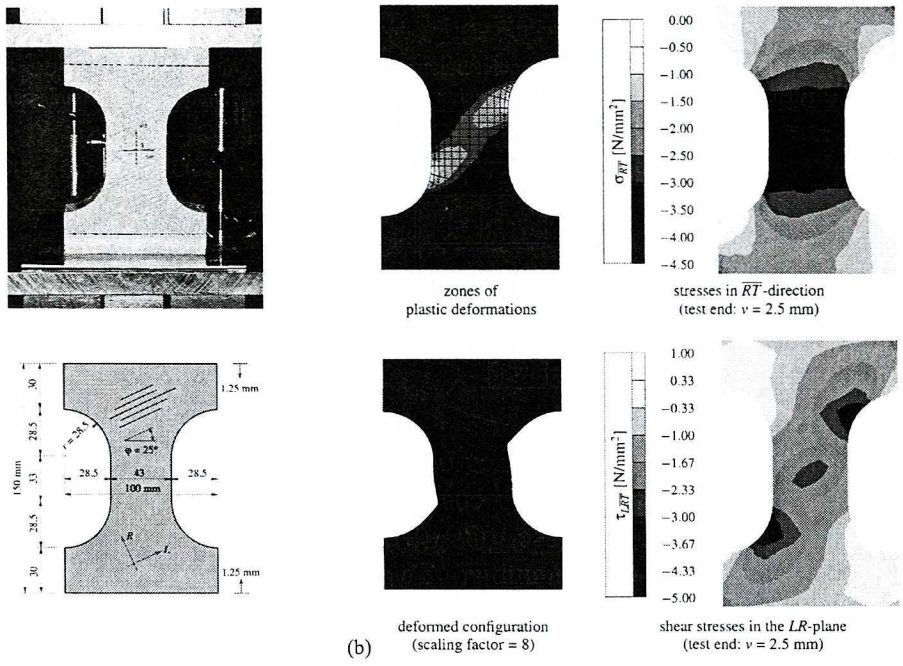

Fig. 11. Comparison of an experiment with a finite element simulation (a) reference configuration and dimensions of the test specimen, (b) results of the finite element simulations

The test specimens have been made of wood of the *LR*-plane of a stem. The elastic material parameters and the five maxima of the strength values for the finite element simulation are summarized in Fig. 12(b).

Figure 12(a) shows a comparison of the load-displacement relationships of the experimental investigations and the results of the numerical simulations performed with the used parameters.

(a)

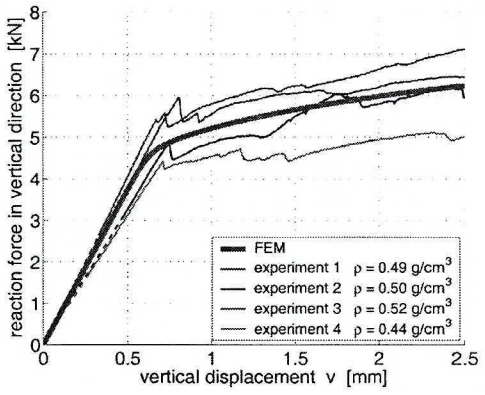

(b)

E_L =	9000 N/mm²
$E_{\overline{RT}}$ =	500 N/mm²
$\nu_{L\overline{RT}}$ =	0.50
$G_{L\overline{RT}}$ =	450 N/mm²
max $\beta_{t,L}{}^0$ =	49.0 N/mm²
max $\beta_{c,L}{}^0$ =	37.0 N/mm²
max $\beta^0_{t,\overline{RT}}$ =	3.4 N/mm²
max $\beta^0_{c,\overline{RT}}$ =	3.0 N/mm²
max $\beta^0_{shr,\overline{RT}}$ =	6.5 N/mm²

Fig. 12. (a) Load-displacement relationship, (b) material parameters for numerical simulation

Full-field displacement analysis with the ESPI-system was not possible, because of the high plastic deformations per displacement step. Thus, the comparison of the displacements of the numerical simulation and the measured deformations was not possible.

However, the results of the numerical simulation show a good agreement with results of the experimental tests. By contemplating the deformed specimen at test end, the zones of plastic deformations agree with the numerical simulations. The critical zones of the test specimen due to vertical displacements have been correctly identified by means of the proposed material model.

5. Conclusions

In this paper an overview on the development of a new constitutive model for the simulation of spruce wood under various biaxial in-plane stresses is presented. The applicability of the model was proven by means of a comparison between an experiment and the corresponding non-linear finite element analysis of a bone-shaped test specimen.

The material model is based on observations from a comprehensive test series for the experimental identification of the failure envelope for clear spruce wood under arbitrary biaxial stress states. Employing this as well as microscopic observations and their macroscopic translation led to the multi-surface plasticity model by MACKENZIE-HELNWEIN et al. [3]. It consists of four surfaces representing four basic failure modes. The separated description of four modes easily enables the modelling of their respective post-failure behaviour.

The more extensive mechanical description inherits the extra mathematical and computational effort for the treatment of edge and corner problems. This leads to the intention to combine the prediction of failure modes with the simplicity of a smooth single-surface model. It can be achieved by tracing a series of strain-type variables, each representing one of the previously introduced scalar hardening and softening parameters.

A significant improvement of this model compared to classical orthotropic stress analysis in combination with a failure envelope is its ability to identify active failure modes. This is achieved by means of the non-associative flow rule. The equivalent strain parameters collected in the vector α are directly linked to the failure mechanisms. Thus, the dominant failure mechanisms of the experiment, perpendicular to grain cell crushing and shear failure in a plane perpendicular to grain, are in good comparison with the experimental results.

The advantages of the proposed formulation are:

- The ability to identify five distinct modes of failure in the material. These modes may be activated individually or as combined failure modes.
- The ability to describe hardening and softening by means of six distinct strength functions. These functions can be experimentally verified and, if needed, easily replaced by almost any characteristic strength function.
- Due to the single-surface description, the effort for the numerical integration of the rate equations by means of the return mapping algorithm remains moderate.
- A closed form expression for a non-symmetric material tangent operator is available. This is important for an effective numerical implementation.

The presented numerical example gave a brief demonstration of the suitability of the presented material model and its numerical implementation. Further numerical studies with experimental verification on model beams are planned for the near future.

Manuscript received by Editorial Board, February 07, 2005;
final version, June 22, 2005

REFERENCES

[1] Eberhardsteiner J.: Mechanisches Verhalten von Fichtenholz – Experimentelle Bestimmung der biaxialen Festigkeitseigenschaften. Vienna, Springer, 2002, in German.

[2] Fleischmann M., Müllner H. W., Eberhardsteiner J.: An Orthotropic Single-Surface Plasticity Model for Spruce Wood under Consideration of Knot Effect. Proceedings of the 21st Danubia-Adria Symposium on Experimental Methods in Solid Mechanics, 2004, pp. 246÷247.

[3] Mackenzie-Helnwein P., Eberhardsteiner J., Mang H. A.: A Multi-Surface Plasticity Model for Clear Wood and its Application to the Finite Element Analysis of Structural Details. Computational Mechanics, 2003, Vol. 31, pp. 204÷218.
[4] Müllner H. W., Mackenzie-Helnwein P., Eberhardsteiner J.: Constitutive Modelling of Clear Spruce Wood under Biaxial Loading by Means of an Orthotropic Single-Surface Model under Consideration of Hardening and Softening Mechanisms. Proceedings of the 2nd International Symposium on Wood Machining, 2004, pp. 83÷90.
[5] Müllner H. W., Mackenzie-Helnwein P., Eberhardsteiner J.: Constitutive Modelling of Biaxially Stressed Wood for the Analysis of Layered Wooden Shells. Proceedings of the 3rd International Conference of the European Society for Wood Mechanics, 2004, pp. 277÷284.
[6] Tsai S. M., Wu E. M.: A General Theory of Strength for Anisotropic Materials. Journal of Composite Materials, 1971, Vol. 5, pp. 58÷80.

Ortotropowy jednopowierzchniowy model plastyczności drewna świerkowego z uwzględnieniem wpływu sęków

Streszczenie

Analiza konstrukcji i elementów konstrukcyjnych metodą elementów skończonych wymaga użycia odpowiednich modeli materiałowych. W chwili obecnej wciąż brak jest tego typu modeli przydatnych dla konstrukcji drewnianych. W Institute for Mechanics of Materials and Structures, Vienna University of Technology prowadzono długookresowy projekt badawczy dotyczący budowy modeli materiałowych. Istotnym punktem wspomnianego projektu było pozyskanie danych o właściwościach mechanicznych drewna świerkowego obciążonego dwuosiowo w kierunku skośnym w stosunku do włókien. Umożliwiło to lepszą symulację stanu naprężeń wieloosiowych w rzeczywistych konstrukcjach drewnianych.

W pracy opisano urządzenia pomiarowe, eksperymenty, zaproponowany model materiału i jego implementację w oprogramowaniu metody elementów skończonych. Użyteczność modelu została wykazana przy użyciu nieliniowej analizy elementów skończonych testowej próbki o kształcie kości.